Received: 26 October 2020 | Revised: 16 July 2021 | Accepted: 27 July 2021

DOI: 10.1111/geb.13377

RESEARCH ARTICLE

Global Ecology and Biogeography | A Journal of Macroecology | WILEY

Growing faster, longer or both? Modelling plastic response of *Juniperus communis* growth phenology to climate change

Jan Tumajer[1,2] | Allan Buras[3] | J. Julio Camarero[4] | Marco Carrer[5] | Rohan Shetti[6] | Martin Wilmking[1] | Jan Altman[7] | Gabriel Sangüesa-Barreda[8] | Jiří Lehejček[6]

[1]Institute of Botany and Landscape Ecology, University of Greifswald, Greifswald, Germany

[2]Department of Physical Geography and Geoecology, Faculty of Science, Charles University, Prague, Czech Republic

[3]School of Life Sciences Weihenstephan, Technical University Munich, Freising, Germany

[4]Instituto Pirenaico de Ecología (IPE-CSIC), Zaragoza, Spain

[5]TeSAF Department, Università degli Studi di Padova, Legnaro, Italy

[6]Faculty of Environment, Julius von Payer Institute for Arctic and Subarctic Research, Jan Evangelista Purkyně University, Ústí nad Labem, Czech Republic

[7]Institute of Botany of the Czech Academy of Sciences, Průhonice, Czech Republic

[8]iuFOR-EiFAB, University of Valladolid, Soria, Spain

Correspondence
Jan Tumajer, Institute of Botany and Landscape Ecology, University of Greifswald, Soldmannstraße 15, 17487 Greifswald, Germany.
Email: tumajerj@uni-greifswald.de

Funding information
Seventh Framework Programme; Alexander von Humboldt-Stiftung; Institute of Botany of the Czech Academy of Sciences, Grant/Award Number: RVO67985939; Grantová Agentura České Republiky, Grant/Award Number: 20-05840Y; Jan Evangelista Purkyne University, Grant/Award Number: UJEP-SGS-2020-44-003-3; Spanish Ministry of Economy, Industry, and Competitiveness, Grant/Award Number: FJCI 2016-30121; Horizon 2020 Framework Programme, Grant/Award Number: 262693 and 730938;

Abstract

Aim: Plant growth and phenology respond plastically to changing climatic conditions in both space and time. Species-specific levels of growth plasticity determine biogeographical patterns and the adaptive capacity of species to climate change. However, a direct assessment of spatial and temporal variability in radial growth dynamics is complicated, because long records of cambial phenology do not exist.

Location: Sixteen sites across European distribution margins of *Juniperus communis* L. (the Mediterranean, the Arctic, the Alps and the Urals).

Time period: 1940–2016.

Major taxa studied: *Juniperus communis*.

Methods: We applied the Vaganov–Shashkin process-based model of wood formation to estimate trends in growing season duration and growth kinetics since 1940. We assumed that *J. communis* would exhibit spatially and temporally variable growth patterns reflecting local climatic conditions.

Results: Our simulations indicate regional differences in growth dynamics and plastic responses to climate warming. The mean growing season duration is the longest at Mediterranean sites and, recently, there has been a significant trend towards its extension of up to 0.44 days/year. However, this stimulating effect of a longer growing season is counteracted by declining summer growth rates caused by amplified drought stress. Consequently, overall trends in simulated ring widths are marginal in the Mediterranean. In contrast, durations of growing seasons in the Arctic show lower and mostly non-significant trends. However, spring and summer growth rates follow increasing temperatures, leading to a growth increase of up to 0.32 %/year.

Main conclusions: This study highlights the plasticity in growth phenology of widely distributed shrubs to climate warming: an earlier onset of cambial activity that offsets the negative effects of summer droughts in the Mediterranean and, conversely, an intensification of growth rates during the short growing seasons in the Arctic. Such plastic growth responsiveness allows woody plants to adapt to the local pace of climate change.

Russian Science Foundation, Grant/Award Number: RSF-17-14-01112; Czech Ministry of Education, Youth and Sports, Grant/Award Number: INTER-EXCELLENCE LTAUSA19137

Handling Editor: Sean Michaletz

KEYWORDS

dendrochronology, drought, growing season, juniper, phenology, plasticity, process-based model, shrub, Vaganov–Shashkin model

1 | INTRODUCTION

Woody plants respond to climate change by modifying the timing and duration of climate-driven biological processes, including photosynthesis (Xia et al., 2015; Xu et al., 2016), gas exchange and transpiration (Frank et al., 2015; Oishi et al., 2010), leaf and shoot phenology (Menzel et al., 2006) and cambial activity (Rossi et al., 2016). The plasticity of phenological and growth processes is largely species specific and has significant consequences for species performance and distribution (Vitasse et al., 2010). Plasticity represents an advantage that can enable widespread species to colonize large areas (Ghalambor et al., 2007; McLean et al., 2014) and to reduce the risks of extinction under environmental change (Rehfeldt et al., 2001; Valladares et al., 2014). Moreover, understanding both temporal and spatial variability in physiological processes is crucial in assessing the net global effects of climate–ecosystem feedback loops (Peñuelas et al., 2009). For instance, because increasing temperatures cause the intensification of both respiration and cambial dynamics, specific terrestrial ecosystems have been reported either to increase (Froelich et al., 2015; Richardson et al., 2009) or to weaken (Buermann et al., 2013; Hu et al., 2010) their net ecosystem productivity. However, the knowledge on species-specific levels of spatial variability and temporal trends in growth dynamics is still insufficient, despite its importance for distributional patterns and long-term adaptability to environmental change.

The understanding of temporal plasticity and spatial variability in cambial dynamics or xylogenesis (i.e., the timing and rate of cell production during the year) is especially important for treeless ecosystems in cold and dry environments, where harsh climatic conditions hinder tree existence (Körner, 2012; Pellizzari et al., 2017). Representing distributional margins of woody plants, these shrubby ecosystems often exhibit high sensitivity to climate change. Indeed, a shrub expansion caused by climate warming or wetter conditions has been reported recently for the Arctic tundra (Myers-Smith et al., 2011; Payette & Filion, 1985), alpine areas (Hagedorn et al., 2014; Hallinger et al., 2010) and dry regions (Caldeira et al., 2015). Moreover, shrub ecosystems host some of the most widespread woody plant species (Adams, 2008; Mao et al., 2010), whose climate–growth responses vary significantly along geographical gradients (Buchwal et al., 2020; Pellizzari et al., 2017; Shetti et al., 2018a). This suggests the ability of cambial dynamics to cope with different local climatic conditions.

The growth conditions of woody plants can be reconstructed or forecast from annual rings on temporal scales from seasons to millennia (Schweingruber, 1996). By analysing tree-ring variables, climatic niches can be described for individual sites, regions and even for the whole hemispheres (Babst et al., 2013; Cook et al., 2020; Harvey et al., 2020), as has been the effect of climate change on the redistribution of climatic constraints (Babst et al., 2019; D'Arrigo et al., 2008). However, ring width integrates growth conditions over several growing seasons (Mäkinen et al., 2002; Peltier et al., 2018), which makes it challenging to assess processes at sub-annual or seasonal temporal resolution. At the same time, there is a lack of sites with > 15 years of data on intra-annual cambial dynamics (Cuny et al., 2015; Delpierre et al., 2019) and, in addition, links between leaf phenology inferred from remote sensing data and cambial phenology might be weak or decoupled (Seftigen et al., 2018). Consequently, the variability of growth dynamics across large spatial scales and multidecadal periods can be assessed at present only by indirect methods using numerical models. The timing and rate of cell division and differentiation are tightly climate driven (Delpierre et al., 2019; Rossi et al., 2016; Vaganov et al., 2006); hence, it might be possible to estimate the timing of growth phenology based on climatic data. Equations calculating parameters of cambial dynamics from the course of the past climate might be calibrated with thresholds estimated using empirical evidence from xylogenesis monitoring (Prislan et al., 2019). Alternatively, ring-width chronologies might be decomposed into intra-annual growth segments using climate-driven process-based models (Guiot et al., 2014; Vaganov et al., 2006). In forward mode, these models can simulate growth rates for each temporal segment based on a given set of climatic conditions. Previously, climate-driven process-based models were used to reconstruct intra-annual growth dynamics for various tree species in cold and dry, but also mild environments (Anchukaitis et al., 2006; Sánchez-Salguero et al., 2017; Shishov et al., 2016). In contrast, they have seldom been used to describe the dynamics of shrub growth (but see Sánchez-Salguero & Camarero, 2020).

Here, we assessed the growth dynamics and climate–growth interactions of the widely distributed shrub *Juniperus communis* L. at 16 sites across Eurasia and Greenland from 39 to 70° N. The individual sites, spread across the Mediterranean, the Arctic, the Alps and the Urals, represent three global ecotones at the margins of the European distribution of woody perennials (dry, cold arctic and alpine tree lines, respectively). The widespread distribution of *J. communis* (Thomas et al., 2007) suggests that this species develops site-specific growth patterns. Moreover, the relatively recent expansion of this gymnosperm to the circumboreal area during periods of climatic instability (4.6–0.3 Ma; Mao et al. 2010) might indicate a significant plasticity to climate changes.

We assembled annual ring-width chronologies of *J. communis* for each site and used the climate-driven process-based Vaganov–Shashkin (VS) model of wood formation (Vaganov et al., 2006) to simulate daily growth rates and cambial kinetics since January 1940. Observed annual growth rates served for the calibration/verification of the models. We assessed temporal trends in simulated growth rates throughout the growing season (to answer the question, "Are junipers growing faster?") and in simulated growing season duration (to answer the question, "Are junipers growing for longer?"). We hypothesized that: (1) intra-annual growth dynamics are highly region specific; (2) regions with dominant temperature control over shrub growth (near Arctic and alpine tree lines) show significant trends towards a longer growing season (Körner, 2012; Rossi et al., 2016) and faster growth rates (Hallinger et al., 2010) resulting from an increase in temperature over the study period; however, (3) in the Mediterranean, where the spring temperature increase is counterbalanced by summer drought intensification (Pellizzari et al., 2017; Sánchez-Salguero & Camarero, 2020), we expect a significant extension of the growing season accompanied, nevertheless, by declining annual growth rates.

2 | MATERIALS AND METHODS

2.1 | Study region

We simulated intra-annual growth dynamics of *J. communis* for 16 sites located in contrasting biomes across Eurasia and Greenland (Figure 1). *Juniperus communis* is the most widely distributed woody plant around the globe. It is an evergreen, long-living shrub that inhabits both dry and cold environments across the Northern Hemisphere (Adams, 2008; Thomas et al., 2007). To characterize its growth dynamics limited by low temperature, we assembled five sampling sites in the Arctic (Greenland, Norway, Sweden and Finland), four sites in the Italian Alps (near oceanic alpine tree line) and three sites along the Urals in Russia (near continental alpine tree line). Predominantly drought-limited growth can be expected in the Mediterranean, where we sampled four mountain sites (three in north-eastern Spain and one in southern Italy). The sites are distributed across broad latitudinal, longitudinal and elevational gradients between 39–70° N, 52° W–65° E and 20–2,300 m a.s.l., respectively.

2.2 | Data collection and processing

All wood samples were taken from prostrate juniper shrubs. Specific sampling strategies and site conditions differed between sites mainly in the number of cross-sections sampled and radii measured (Table 1; Supporting Information Table S1). To ensure compatibility of datasets among sites, we used cross-dated series of ring widths representative of individual shrubs. To do this, we averaged series first from radii to cross-sections and, in the next step, from cross-sections to individual shrubs. Biological growth trends from ring-width series were removed using a flexible spline with 50% frequency cut-off at 30 years. This approach retains only high-frequency variability and removes most of the mid- and low-frequency trends (Cook & Peters, 1981). Finally, mean standard site chronologies were obtained by biweight robust averaging of individual detrended series. To ensure representative sample depth for subsequent analyses, each chronology was cropped to contain only the period since 1940. All steps of the processing of ring-width data were performed in R v.3.6.3 (R Core Team, 2020) using the "dplR" package (Bunn, 2008).

Daily mean temperature and precipitation totals were obtained for each site from the CRU JRA 1.1 gridded database with 0.5° resolution (Harris, 2019). For all sites, there were significant trends towards higher temperatures over the last decades (Supporting Information Figure S1). The Mediterranean and the Alps have experienced the greatest increase in temperature during the summer (June–August), whereas the Arctic and the Urals have seen an increase in temperature mainly in winter and spring (January–May). Although some sites in the Arctic have experienced a significant increase in precipitation, the other three regions exhibit mostly non-significant trends.

2.3 | Reconstruction of daily growth dynamics using a process-based model

We used two working blocks of the VS model (Vaganov et al., 2006) to simulate daily values of dimensionless growth functions in the response to climate ("environmental block") and daily dimensions, growth rates and states of cambial cells ("cambial block"). The model inputs include daily resolved temperature and precipitation, with site latitude used to estimate the intra-annual trend in daylength. Daily soil water content is calculated using balance equations reflecting processes of precipitation, interception, drainage, evapotranspiration and snow dynamics (Thornthwaite & Mather, 1955). Site-indexed chronology represents additional mandatory input that might be used for quantifying the model precision and, alternatively, iterative tuning of the site-specific parameters (used as a target variable to maximize the coherence between the simulation and the target; Shishov et al., 2016). For the purpose of this study, we used the versions of the VS model implemented in VS-Oscilloscope (Shishov et al., 2016) and MATLAB code made available by Anchukaitis et al. (2020). Before running the analysis, we identified small differences between both implementations and modified the latter to be consistent with the former (mainly related to the definition of the growing season cessation and the soil moisture model).

In the first step of the environmental block, the VS model estimates partial growth rates (non-dimensional functions of growth limitation) in relationship to temperature (Gr_T) and soil moisture (Gr_M) for each day. The piecewise functions of temperature and moisture growth limitation (Figure 2a) are defined by the groups of four parameters: threshold daily temperature/soil moisture below (T_1/M_1) or above which (T_4/M_4) growth cannot be sustained; and lower (T_2/M_2) and upper (T_3/M_3) margins of temperature/moisture

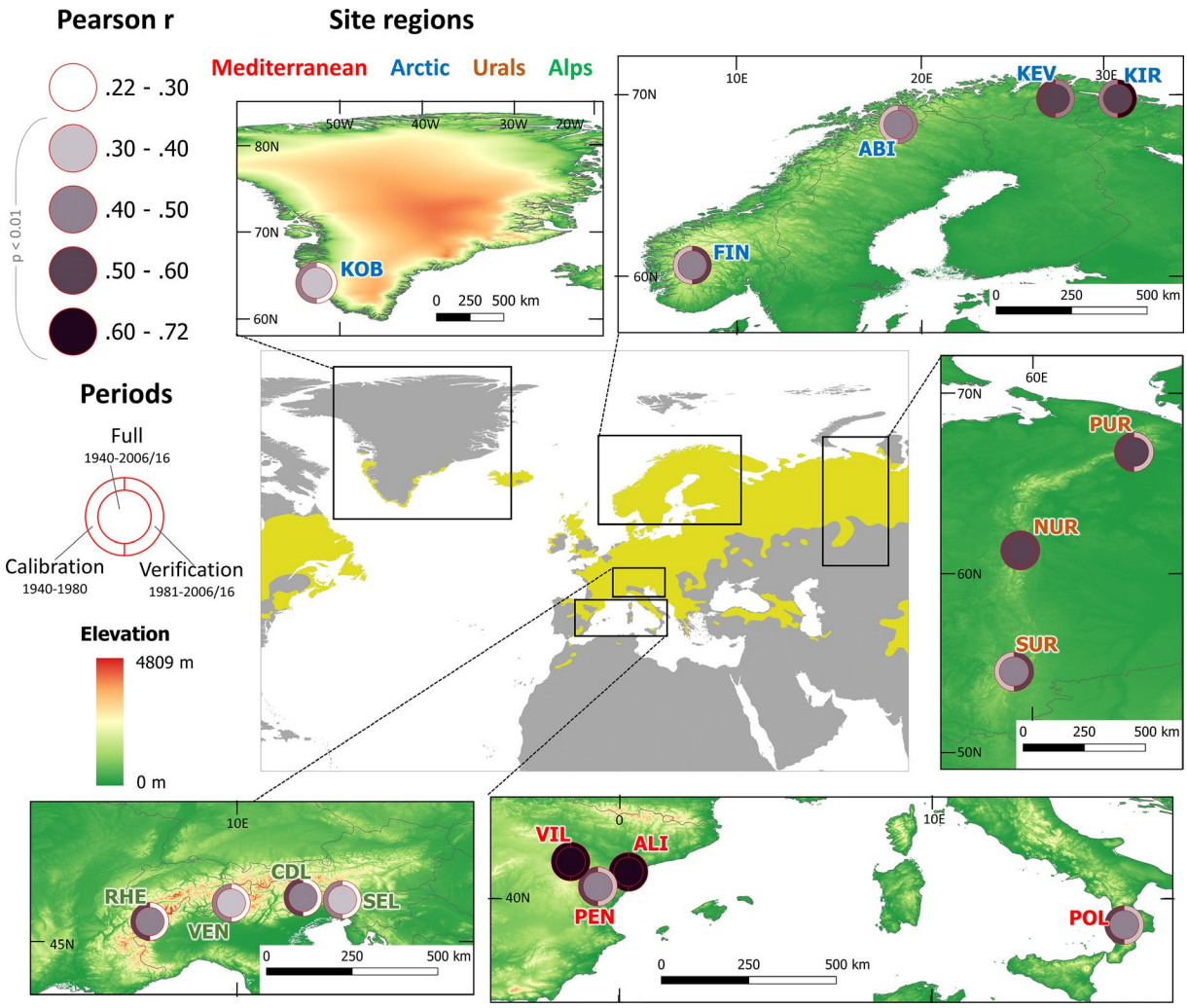

FIGURE 1 Overview of sampling sites. The colour scale indicates the correlation between the observed and simulated ring-width chronology during the specific period. The yellow area in the inset indicates the native range of *Juniperus communis* (according to Caudullo et al., 2017). For site codes, see Table 1

optimum. In addition to climatic partial growth rates, the VS model also estimates, for each day, the partial growth rate to photoperiod (Gr_E) as the ratio of daylength to the daylength of the summer solstice calculated from the site latitude (Figure 2b). Integral daily growth rate (Gr_{INT}) is calculated as the minimum of partial growth rates in relationship to temperature and moisture multiplied by Gr_E (Figure 2c).

Dimensionless daily Gr_{INT} represents the final output of the environmental block and single input into the cambial block, where position-specific radial growth rates (V_j) are determined for theoretical cambial cells aligned in radial file (Figure 2d). Cambial block is activated only during the growing season, with the onset and cessation delimited using the heat-sum approach (Rossi et al., 2016) as the first/last day when the cumulative temperature (Tbeg) during a specific number of preceding days (tbeg) exceeds a specific threshold. According to V_j and the position inside the cambial zone, three possible fates are determined for each cell each day: radial growth inside the cambial zone; differentiation (i.e., transition from the cambial zone to the differentiation zone); or dormancy. Cells forming the cambial zone grow proportionally to V_j until they reach a threshold size to enter the mitotic cycle and divide. Finally, simulated tree ring-width chronology might be determined as the normalized annual sum of Gr_{INT} (Tychkov et al., 2019; Figure 2e) or the normalized number of differentiated tracheids (Anchukaitis et al., 2020). We used the former approach in the present study, owing to similar variance of the simulated chronologies to observed site chronologies. However, there was a strong correlation between both types of simulated chronologies (mean Pearson's $r = .89$, $R^2 = .79$, d.f. = 71, $p < .001$).

The VS model has an intermediate complexity in the representation of processes controlling wood formation (Guiot et al., 2014), building on the assumption of multiple nonlinearities in the response of cambial activity to temperature, soil moisture and photoperiod (Vaganov et al., 2006). As a sink-oriented model, it focuses on the cambial activity (Körner, 2015) but ignores the importance of the rate of photosynthesis (e.g., CO_2 concentration, stomatal regulation), distribution of growth across tree compartments or tree/shrub physiological acclimatization. In addition, simulation outputs hold for

TABLE 1 Basic statistics of site chronologies and the coherence statistics between simulated and observed chronologies

Region	Site code	Site name	Number of individuals	Last ring	rbar	Correlation (R^2) between observed and simulated chronologies		
						Full period (1940–2006/16)	Calibration period (1940–1980)	Verification period (1981–2006/16)
Mediterranean	ALI	Aliaga	15	2016	.429	.64 (.41)	.69 (.48)	.60 (.36)
	PEN	Peñarroya	13	2015	.213	.42 (.18)	.50 (.25)	.35 (.12)
	POL	Pollino	16	2014	.204	.44 (.19)	.53 (.28)	.30 (.09)
	VIL	Villarroya de los Pinares	12	2014	.305	.66 (.44)	.63 (.40)	.71 (.50)
Arctic	ABI	Abisko	52	2006	.047	.42 (.18)	.38 (.14)	.48 (.23)
	FIN	Finse	7	2011	.222	.43 (.19)	.31 (.10)	.55 (.30)
	KEV	Kevo	29	2012	.161	.50 (.25)	.52 (.27)	.49 (.24)
	KIR	Kirkenes	53	2013	.090	.53 (.28)	.48 (.23)	.62 (.38)
	KOB	Kobbefjord	41	2013	.197	.32 (.10)	.44 (.19)	.24 (.06)
Urals	PUR	Polar Urals	20	2013	.302	.50 (.25)	.57 (.32)	.37 (.14)
	NUR	Northern Urals	22	2014	.288	.55 (.30)	.59 (.35)	.54 (.29)
	SUR	Southern Urals	15	2010	.253	.42 (.18)	.38 (.14)	.53 (.28)
Alps	CDL	Croda da Lago	23	2012	.153	.40 (.16)	.54 (.29)	.29 (.08)
	SEL	Sella Nevea	24	2013	.260	.39 (.15)	.43 (.18)	.23 (.05)
	VEN	Val Ventina	75	2016	.240	.35 (.12)	.43 (.18)	.23 (.05)
	RHE	Val di Rheme	17	2014	.250	.40 (.16)	.52 (.27)	.22 (.04)

Note: The rbar is the mean inter-series correlation.

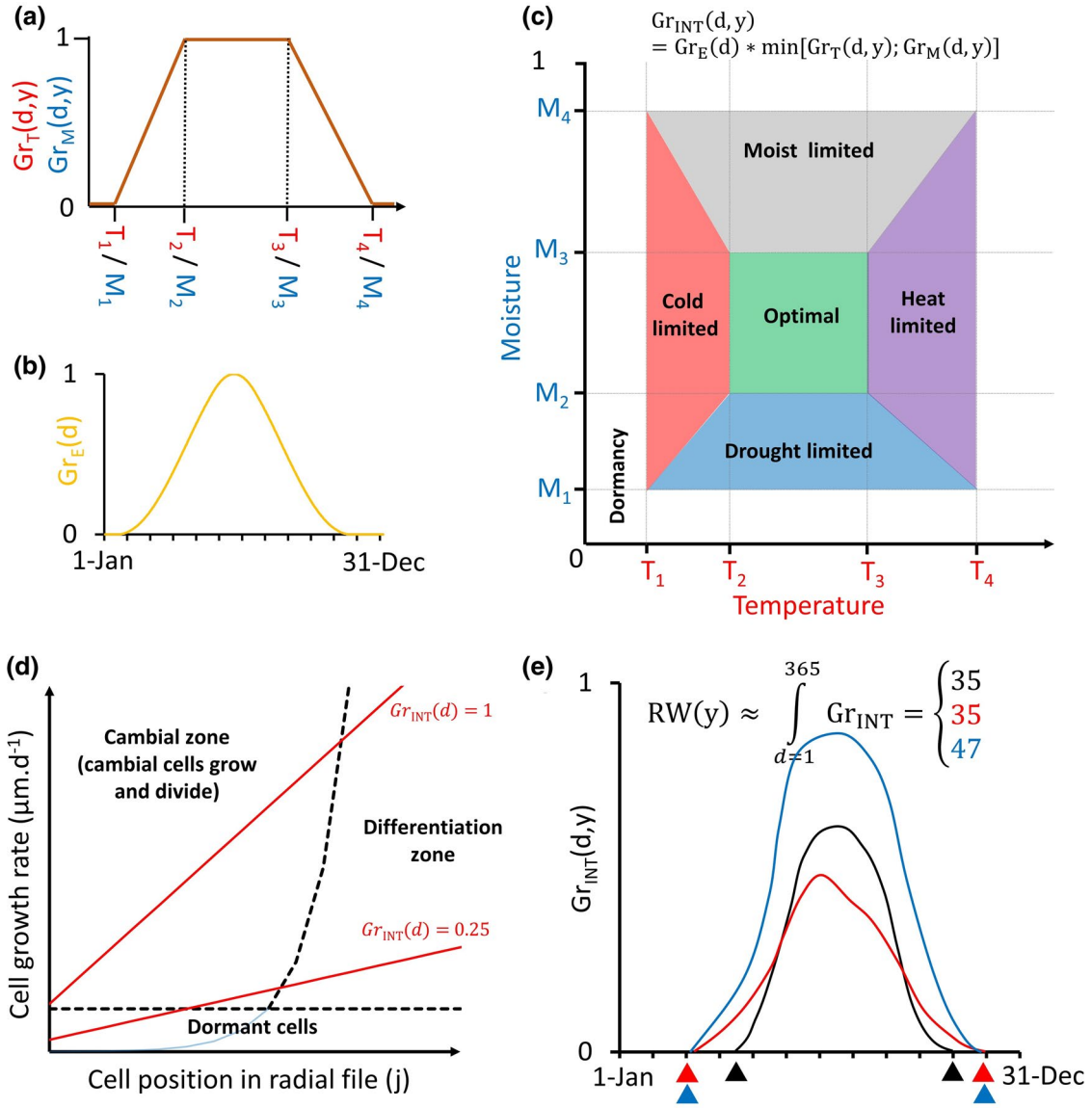

FIGURE 2 Visual representation of the Vaganov–Shashkin model algorithm. (a) The shape of response functions converting daily temperature and soil moisture into dimensionless partial growth responses to temperature/soil moisture. (b) Intra-annual pattern of the ratio of daylength to daylength of the summer solstice (example for the site located at latitude 69.75° N). (c) The equation used to calculate the integral growth rate and classification scheme of days based on the dominant climatic limiting factor. (d) Determination of position-specific cell growth rates and three possible daily "fates" for each cambial cell inside radial file for two theoretical days with different values of Gr_{INT}. (e) Visual representation of hypothesized changes of the past intra-annual pattern of Gr_{INT} attributable to climate change. Triangles indicate the onset and cessation of the growing season determined using the cumulative-temperature threshold. The past pattern of Gr_{INT} is indicated by the black line, and red and blue lines represent hypothesized shifts towards "longer but not faster" and "longer and faster" growth, respectively. Abbreviations: d, day; Gr_E, ratio of daylength to daylength of summer solstice; Gr_{INT}, integral daily growth rate; Gr_T and Gr_M, partial daily growth rates to temperature and soil moisture; j, relative position of the cell inside radial file; *M*, soil moisture; RW, annual ring width; *T*, temperature; y, year

an idealized site-specific average tree regardless of its dendrometry and social status but might not be attributable to individual trees or shrubs at sites with complex stand demography. Consequently, the correlations between observed and simulated annual ring-width chronologies for coniferous tree species typically span between .50 and .70 (Anchukaitis et al., 2006; Evans et al., 2006; Yang et al., 2017), hence capturing between .25 and .50 of observed variability in chronology.

2.4 | Vaganov–Shashkin model calibration

The VS model parameters at specific site might be set to previously justified default values (Evans et al., 2006; St. George et al., 2008) or iteratively tuned against local site chronologies (Shishov et al., 2016). To balance high between-site variability in growth conditions but restrict the number of variable parameters, we set all the parameters of the cambial block and most parameters of the soil moisture model

to their defaults (Evans et al., 2006; Vaganov et al., 2006). In contrast, we iteratively tuned 13 parameters to maximize the correlation between observed and simulated chronologies using VS-OSCILLOSCOPE (Shishov et al., 2016). Tuned parameters included response functions parameters (T_1–T_4 and M_1–M_4), threshold cumulative temperature and period to onset/cease cambial activity (Tbeg and tbeg), rooting depth (Ir), drainage coefficient (Λ) and initial soil moisture (M_0). The choice of tuned parameters reflected previous studies showing high sensitivity of the simulated chronology to variation of the specific parameters (Anchukaitis et al., 2020; Tumajer et al., 2021; Tychkov et al., 2019).

We adopted the three-stage approach presented by Büntgen et al. (2021) to quantify temporal stationarity of the model parameters. Initially, we performed iterative calibration of tuneable parameters for the period 1940–1980 to maximize the correlation between observed and simulated chronologies. Next, the calibrated parameters were used to simulate growth during the 1981–2006/2016 independent verification period (for the last years of individual sites, see Table 1). We assessed the stationarity of the parameters by: (1) comparing correlation coefficients between observed and simulated chronologies for calibration and verification periods; and (2) using a bootstrapped transfer function stability test (Buras et al., 2017). The latter approach estimates parameters of a linear regression (intercept, slope and R^2) between simulated and observed ring-width chronologies for both calibration and verification subperiods and quantifies the overlap of their bootstrapped confidence intervals. We were not able, inversely, to set the late period for calibration and the early period for verification, because the VS model assumes mechanistically that dormant cambium at the end of the year determines the initial status of the cambial zone in the following year (Anchukaitis et al., 2020; Vaganov et al., 2006). After quantifying temporal stability on the independent verification period, we slightly adjusted calibrated parameters to maximize simulation coherence with observed chronologies during the entire 1940–2006/2016 period. This approach both enables the assessment of temporal stationarity of parameters and maximizes the robustness of the response function over the full period. However, the final calibration is not fully independent of the tuning process, and the final simulations assume variable levels of consistency with observations (indicated by R^2). By using the single final set of constant parameters over the full period, we assume that there is a strong physiological control determining threshold values of growth response to the environment (Rathgeber et al., 2016; Rossi et al., 2008), while acclimatization or evolutionary processes resulting in possible shifts of those thresholds are marginal over the considered timespan (Evans et al., 2006; Vaganov et al., 2006).

2.5 | Simulated growing season phenology and kinetics

We extracted the following data from the VS model outputs: simulated ring-width chronologies; daily values of simulated growth rates (Gr_{INT}, Gr_T and Gr_M); daily numbers of cells transiting from the cambial zone into the differentiation zone; and days of the year (DOY) with onset/cessation of cambial activity. To assess trends in climatic limitation of growth rates, we calculated slopes of linear trends in Gr_T, Gr_M and Gr_{INT} for each DOY since 1940. Likewise, we quantified trends in simulated chronologies and in the duration of the growing season (determined as the number of days between onset and cessation of cambial activity). To quantify the cell differentiation rate during the year, we calculated the number of cells differentiated per day in 15-day moving windows shifted by 1 day. Trends in cell differentiation rate since 1940 were assessed for each DOY using linear regressions.

To describe between-site similarities in climatic limiting factors, we performed hierarchical clustering of sites based on their monthly means of Gr_T and Gr_M (24 parameters for each site). Monthly means were preferred instead of simulated daily values to prevent overfitting. The hierarchical clustering delineates nested groups of sites and identifies similarity thresholds (Ward average-link method was applied here) between individual nests where the theoretical grouping changes (Rokach & Maimon, 2005).

2.6 | Vaganov–Shashkin model robustness

Vaganov–Shashkin model simulations represent an estimate of intra- and inter-annual juniper growth, because the model reflects only climatic variables and their nonlinear effects on cambial dynamics (Vaganov et al., 2006). We performed a set of verification exercises to quantify the robustness of the simulations. To verify whether the simulated tracheid numbers reflect between-site variability in mean ring widths, we regressed site mean numbers of cells produced per year (simulation) against mean raw ring width (observation). Likewise, we regressed trends in simulated ring widths against trends in observed raw chronologies.

In addition to comparing simulated and observed site chronologies, the VS model output can be compared against xylogenesis data to assess the precision of simulated intra-annual growth phenology and kinetics (Buttò et al., 2020; Tumajer et al., 2021). We compared the simulated intra-annual pattern of tracheid number with xylogenesis observations of *J. communis* at the PEN site located in eastern Spain (Figure 1) during 2014. To the best of our knowledge, *J. communis* xylogenesis monitoring does not exist for any of the other study sites. The comparison of the simulations with a single year of observations is informative but does not provide a full verification of the intra-annual performance of the model. In addition, a single year of xylogenesis observations does not permit a validation of inter-annual variability in the duration of the growing season.

3 | RESULTS

Chronologies simulated by the model calibrated during the full period of 1940–2006/2016 were significantly ($p < .01$) correlated

with observed chronologies for all 16 sites (Figures 1 and 3). The values of the model parameters are listed for each site in the Supporting Information (Table S2). Correlations (R^2) between observed and simulated chronologies vary between .32 and .66 (.10–.44). The greatest model coherence is observed in the case of the Mediterranean [mean correlation .54 (.29)], followed by the Urals [.49 (.24)] and the Arctic [.44 (.20)]. In contrast, the model outputs for the Alps are less skilful [.38 (.15); Table 1]. The mean correlations (R^2) for simulations based on independent calibration (1940–1980) and verification (1980–2006/2016) periods equalled .50 (.26) and .42 (.20), respectively (Figure 1; Table 1). Correlations were > .3 for all sites in the calibration period. In contrast, correlations dropped below this threshold for the KOB site in the Arctic and all sites in the Alpine region during the verification period. Bootstrapped transfer function stability tests indicated temporal stability of all regression components for most of the sites (Supporting Information Table S3).

Simulated intra-annual growth patterns differ considerably between the regions (Figure 4). Three different types of sites can be distinguished based on the simulated dominant climatic limiting factor during the growing season: low temperature (the Arctic, the Northern and Polar Urals); drought (the Mediterranean and the Southern Urals); or high soil-moisture content (Eastern Alps; Figure 4; Supporting Information Figure S2). The growing season lasts on average 237 days in the Mediterranean region, with only spring and autumn (approximately before DOY 150 and after DOY 300) being predominantly temperature limited. During the middle of the growing season, growth rates are restricted by low moisture availability. In contrast, the Arctic experiences short growing seasons (109 days on average). Cambial activity is limited almost exclusively by low temperatures in this region, with only occasional occurrence of days with drought or moist limitation or climatically optimal conditions. The growth dynamics of *J. communis* in the Northern and Polar Urals are restricted by low temperatures during spring and autumn and by soil moisture variation in summer. In contrast, drought limitation dominates in the southern Urals. The average duration of the growing season in the Urals is 116 days and declines with increasing latitude. Finally, the model suggests a growth limitation by the moist conditions for sites in the Eastern Alps (mainly SEL and partly CDL) and by suboptimal soil moisture in the Western Alps (VEN and RHE). The mean simulated duration of the growing season in the Alps is 151 days.

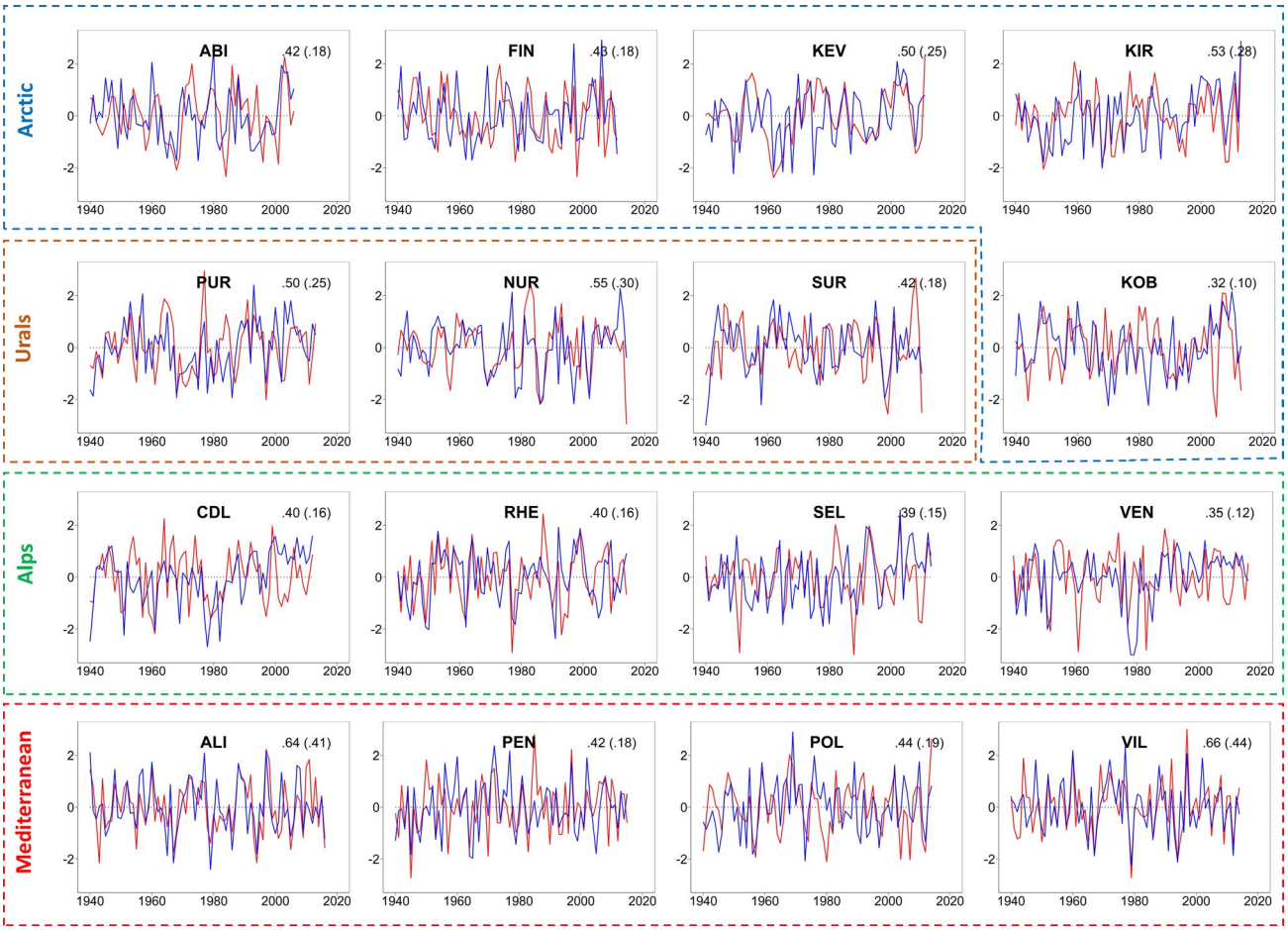

FIGURE 3 Comparison between observed (red) and simulated (blue) site-indexed ring-width chronologies. The *x*-axes indicate years, and *y*-axes show indexed simulated and observed ring widths. The statistics in the top right corner of each panel indicate the Pearson correlation coefficient between simulated and observed chronologies (respective R^2 of linear model). All correlations are significant ($p < .01$). For site codes, see Table 1

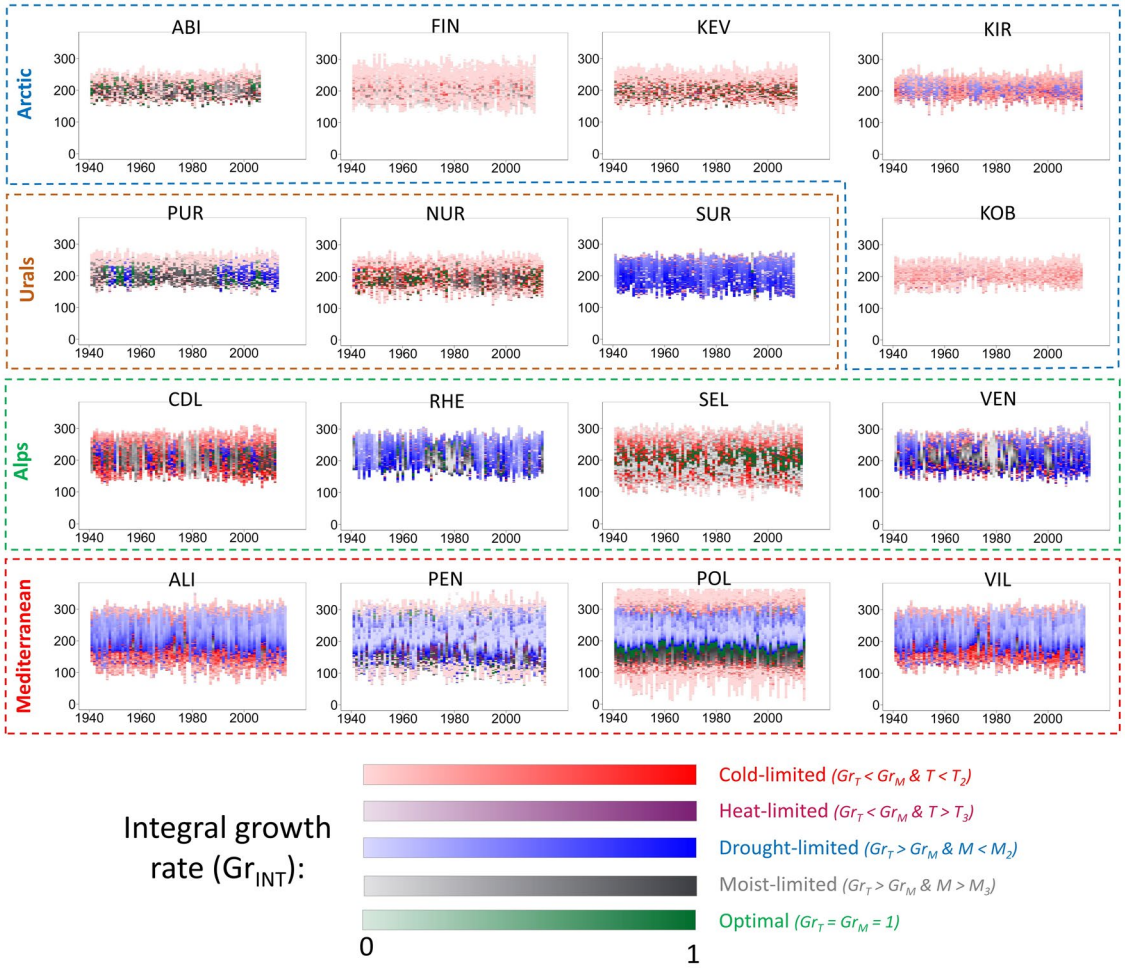

FIGURE 4 Outputs of the Vaganov–Shashkin model on a daily scale. Matrices present the integral growth rates (Gr_{INT}), indicated by the colour scale, for each day (rows) and year (columns). Colours depict the climatic parameter with dominant control over cambial activity each day. For site codes, see Table 1. Abbreviations: Gr_M, partial growth rate to soil moisture; Gr_T, partial growth rate to temperature; *M*, soil moisture; *T*, temperature

Simulated integral growth rates (Gr_{INT}) and simulated rates of tracheid differentiation during sequential independent 15-day windows show coherent intra-annual patterns and trends (Figure 5; Supporting Information Figures S3–S5). Both simulated variables experience positive trends during early summer (before DOY 160) and, in part, also during late autumn (after DOY 300) at Mediterranean sites, which is driven by increasing temperature (Gr_T). However, growth rates drop during summer because of a decline in soil moisture (Gr_M). Consequently, none of the sites in the Mediterranean exhibits any significant trend in simulated ring width (trends vary between −0.06 and 0.10 %/year; mean 0.01 %/year). In the Arctic, simulated integral growth rates and the smoothed cambial kinetics during summer couple positive trends in Gr_T. Although those trends for individual DOYs mostly lack statistical significance, when cumulated over the entire year they result in simulated ring-width increase of 0.01–0.32 %/year (on average, 0.17 %/year). The trend in annual growth rates is statistically significant at the KIR site in the Arctic. In the Urals, growth rates generally increase before DOY 180–200, being driven by increasing Gr_T, but they decline afterwards because of decreasing Gr_M owing to drought (SUR) or marginally decreasing Gr_T owing to temperature decline (PUR). Cumulatively, the trend in simulated ring width shows a latitudinal gradient from −0.04 %/year at the SUR site (southern Urals) to 0.25 %/year at the PUR site (Polar Urals). Increases of integral growth rates and simulated cell differentiation rates per 15-day window occur across the entire growing season in the Eastern Alps (sites SEL and CDL). In contrast, the trends in summer Gr_{INT} are mostly non-significant in the Western Alps (sites VEN and RHE). Trends in simulated ring width span between 0.11 and 0.52 %/year (on average, 0.32 %/year) in the Alps.

Model simulations suggest statistically significant trends in growing season duration for eight of sixteen sites (Supporting Information Figure S6). The steepest trends in growing season duration were found for the Mediterranean sites, where the slopes of linear regressions reach up to 0.44 days/year (three of four sites with $p < .01$). Likewise, a significant positive trend was simulated for the dry Southern Ural (SUR) site of 0.17 days/year. Significant trends were also documented for three sites in the Alps (0.19–0.30 days/year) and the FIN site in the Arctic (0.21 days/year).

The observed progress of tracheid formation is tightly synchronized with simulations during the growing season of 2014 at the

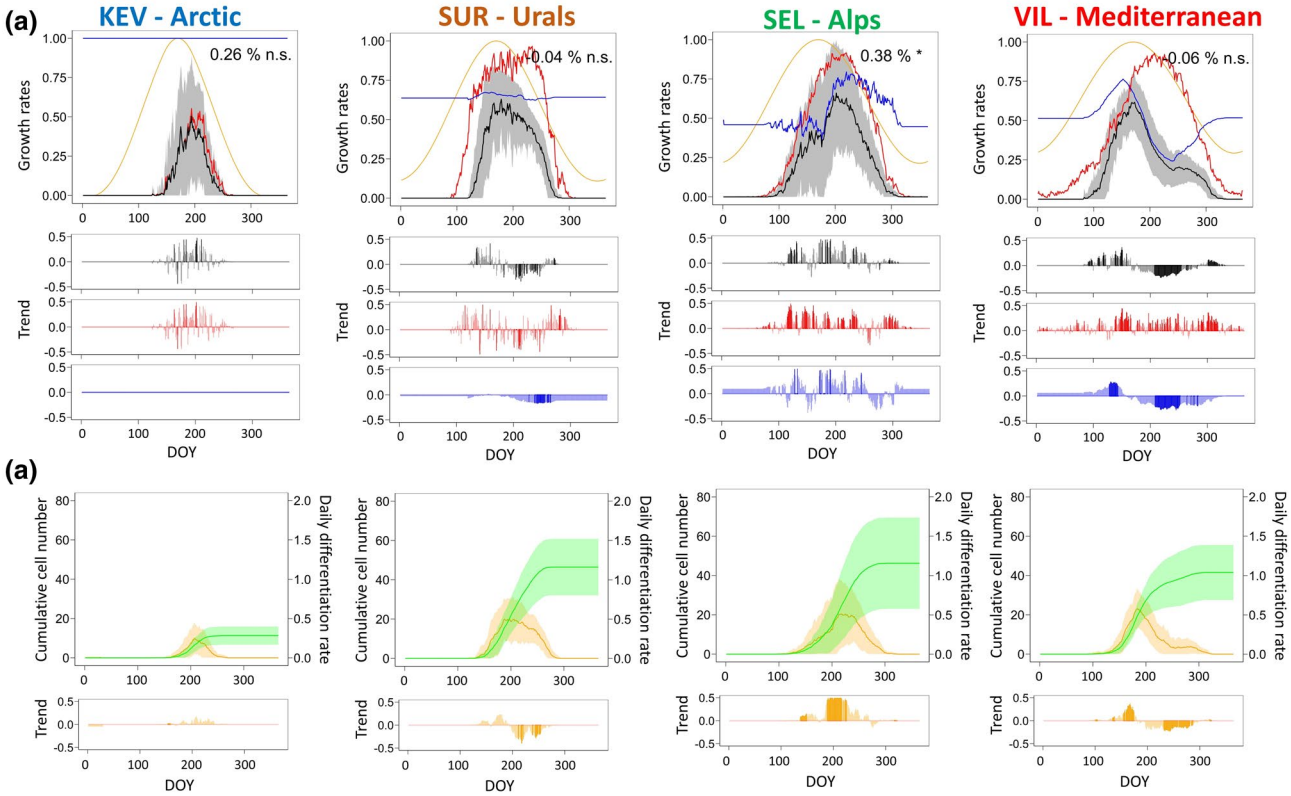

FIGURE 5 Mean intra-annual patterns and linear trends of (a) simulated dimensionless growth rates, and (b) cumulative differentiated cell numbers and mean daily differentiation kinetics during subsequent independent 15-day windows since 1940. One representative site is shown for each region; for other sites, see the Supporting Information (Figures S3–S5). Mean intra-annual patterns in growth rates, cell numbers and cell differentiation kinetics since 1940 are shown in line charts in the upper parts of both panels, and their linear trends per 100 years for each day of year (DOY) are shown as bar charts in the bottom parts of both panels. Colours refer to partial growth rate to temperature (red), partial growth rate to soil moisture (blue), partial growth rate to daylength (yellow), integral growth rate (black), cumulative number of differentiated cells (green) and daily rate of cell differentiation (orange). Buffers indicate ±*SD*. Significant trends ($p < .05$) are denoted as filled bars. Percentages annotated in the top right corner of (a) indicate trends in cumulative annual integral growth rates per year (*$p < .05$; n.s. $p > .05$)

PEN site (Supporting Information Figure S7). Site means of raw ring widths and simulated cell numbers and slopes of their trends are positively but non-significantly correlated in both cases (Supporting Information Figure S8).

4 | DISCUSSION

4.1 | Geographical patterns and trends in juniper growth phenology

Our simulations of *J. communis* wood formation demonstrate pronounced regional differences in growth dynamics and in its responsiveness to climate change.

Simulated growth dynamics for Mediterranean sites reflect the bimodality of both primary (Montserrat-Martí et al., 2011) and secondary (Camarero et al., 2010) meristem activity typical for this region. The growth is characterized by a very early start of the growing season, growth maximum during late spring, suppressed growth in summer, a second growth maximum during autumn, and winter dormancy. Moreover, the VS model suggests a significant redistribution of seasonal growth rates, most probably owing to climate change, leading to shifting bimodality and enhancing the amplitude between spring/autumn and summer growth rates. Most apparently, growth rates decline during summer months because of reduced soil moisture. However, the temperature-driven increase of spring and autumn growth rates, together with the extension of the growing season, counterbalance the negative effect of increasing summer drought stress on total growth over the entire growing season. Consequently, simulated ring widths exhibit rather stable trends since 1940. Our results suggest that the earlier start of radial growth in junipers compared with coexisting trees in drought-prone Mediterranean mountains (García-Cervigón Morales et al., 2012) might be a factor determining their better performance under recent climate change (Pellizzari et al., 2017). With an earlier onset of growth, *J. communis* can form a significant part of the annual ring during spring, when water availability is not a limiting factor, and rising temperatures affect growth positively. For the same reason, however, the growth of Mediterranean shallow-rooting juniper shrubs becomes

highly sensitive to winter–spring dry spells (Sánchez-Salguero & Camarero, 2020).

The growth of *J. communis* in the Arctic is controlled by temperature, with marginal importance of drought or high soil moisture limitation restricted to the driest (KIR) and wettest (ABI) sites, respectively. Simulated cambial dynamics suggest a very short growing season, with a single peak in growth rate synchronized with the annual temperature maximum around the summer solstice. The mean simulated growing season duration in the Arctic is 109 days, which is similar to the global minimum for tree line existence (94 days; Körner, 2012). Both the very short length of the growing season and the low simulated growth rates explain the dominance of shrubs over trees throughout most of the Arctic tundra. Shrubs can sustain a growing season of 45 days and require smaller amounts of new biomass to persist each year (Körner, 2012). Although the VS model suggests trends towards wider rings on average of 0.17 %/year, surprisingly, the mean trend in simulated growing season duration is only 0.06 days/year in the Arctic. This stands in contrast to studies reporting an extension of the growing season through the Arctic from both remote sensing and *in situ* data (Chae et al., 2015; Weijers et al., 2013). This can be linked to differences in cambial and leaf phenology (Sass-Klaassen et al., 2011) and different spatial extents of their estimates (site-specific cambial phenology vs. areally extensive leaf phenology derived from remote sensing; Seftigen et al., 2018). In addition, there are weak trends in June temperature, which probably plays a key role in the timing of the onset of cambial activity in the Arctic. Trends for all Arctic sites span between 0.001 and 0.01 °C/year, apparently resulting in a weak stimulation of earlier growth onset in cold regions (Rossi et al., 2008). Further research should verify whether the "Arctic greening" inferred from remote sensing data (Myers-Smith et al., 2011) corresponds to a longer growing season or higher growth rates of tundra shrubs.

The Urals span a wide latitudinal climatic gradient; hence, intra-annual growth patterns vary significantly between sites, because the environmental conditions controlling growth differ (Shetti et al., 2018a, 2018b). The southernmost site, SUR, is characterized by dominant drought limitation in summer. With increasing latitude, the importance of drought control over cambial activity declines. This is in line with differences in climatic signal determined using linear methods; the chronologies for the NUR and PUR sites are positively correlated with temperature, whereas the response of the SUR chronology is non-significant or even negative (Shetti et al., 2018b). Moreover, individual sites in the Urals experience the redistribution of growth rates during the year because of climate change in different ways. As for the Mediterranean region, growth rates at the SUR site increase during the early parts of the growing season (DOY 150–180) and decline in the moisture-limited season (DOY 200–280). In addition, significant extension of the growing season was simulated at the SUR site. Growth rates at the PUR site also increase during the early part of the growing season and decrease after DOY 220. The most likely reason for those decreases, contrary to drying at the SUR site, resides in slightly decreasing mean August temperature (−0.005 °C/year; Supporting Information Figure S1) and stable mean summer temperatures (Hagedorn et al. 2014) in the northern Urals. Declining August temperatures were counterbalanced by increases in spring growth, because the model suggests a 0.25 %/year increase in ring widths for the PUR site. As a consequence, the tree line in the Urals is an exceptional cold-limited environment, because the elevational expansion of woody plants (Hagedorn et al., 2014) and increasing annual growth rates (as we show here) seem to occur without a concurrent increase of summer temperatures and depend more on winter snowfall dynamics and spring temperatures.

In comparison to the Mediterranean, the Urals and the Arctic, the VS model showed suboptimal results in the Alps. Although the simulations were highly correlated with observed chronologies over calibration and full periods, they dropped for independent verification subperiods. Sites in the Eastern Alps, but not in the Western Alps, experienced a pronounced limitation of summer growth dynamics by high soil moisture, which agrees with the observed pattern of negative precipitation–growth correlations (Carrer et al., 2019). The simulated negative response to high soil moisture might reflect both direct effects of soil anoxic conditions on respiration typical for wet ecosystems (Pallardy, 2008) and indirect effects of shifting cambial phenology by snow dynamics (Carrer et al., 2019), evaporative cooling of surface temperatures (Pellizzari et al., 2014) or cloudiness–temperature interactions. However, suboptimal levels of correlation coefficients and temporal non-stationarity of model parameters indicate that some additional processes important for juniper growth in the Alps remain neglected in the model. Consequently, although the outputs of the models seem realistic in terms of existing knowledge on local xylogenesis (Rossi et al., 2007) and the negative effect of winter precipitation on Alpine shrub growth (Carrer et al., 2019), they should be treated with caution.

4.2 | Limitations of process-based modelling of juniper growth

By using a process-based model of moderate complexity, we were able to estimate intra-annual growth dynamics along broad climatic gradients from dry, wet to cold environments. The simulated and observed chronologies were correlated significantly at all sites, and the mean correlation was .46 (.48 excluding the Alpine sites). Mean correlations obtained during the independent calibration-verification exercise were .50 and .42, respectively. Those statistics are comparable to the largest study using the default VS model parameters on the Northern American tree-ring chronologies preferentially sampled in areas with a strong climatic signal for palaeoclimatic reconstructions (Evans et al., 2006). This indicates that sites included in our network represent the contrasting ecological limits of *J. communis* distribution.

Although the simulated and observed chronologies were significantly correlated at all sites, the mean coherence and stationarity differed substantially between regions. The correlation coefficients were the highest in the Mediterranean and the lowest in the Alps, where the model also presented pronounced non-stationarity. The

variable model performance in contrasting environments limits its applicability in large-scale network studies because it leads to a variable level of confidence for the ecological interpretations of the simulations in different regions. Indeed, we obtained only limited support for the simulated intra-annual growth pattern and its response to climate change in the Alps, although the negative interaction between moisture and growth in the Eastern Alps accords well with existing knowledge (Carrer et al., 2019; Pellizzari et al., 2014). We suggest that the future development of simple climate-driven process-based models should focus on identification and implementation of additional region-specific mechanisms of climate–growth interaction to ensure similar skills of the model across contrasting environments while, however, keeping the model relatively simple in terms of input data requirements.

We are aware that because of the climate-driven algorithms of the VS model, simulated intra-annual patterns do not represent the entire variability in growth dynamics, but purely its climatic component (Kirdyanov et al., 2020). In other words, simulated trends in growth phenology and kinetics fully mirror the trends in climatic data. Disturbance agents might explain specific, unusually high residuals between simulated and observed ring-width chronologies, such as extensive defoliator outbreaks and associated greater herbivore pressure on non-preferred browsing plants during 2004–2005 at the KOB site in Greenland (Prendin et al. 2020; Wilmking et al. 2018; Figure 3). The suboptimal performance of the model at some sites might indicate locally high importance of non-climatic processes or non-stationary responses of growth to climate. The simulation–observation coherence might have been reduced by the solar dimming in the Arctic (D'Arrigo et al., 2008) or by dieback events in the Mediterranean and associated shifts in stand structure and composition (Sánchez-Salguero & Camarero, 2020). Moreover, as a purely climate-driven model, outputs of the VS model are sensitive to the quality of the daily climatic data, which, in the case of CRU JRA datasets, might show inhomogeneities before 1958 (Harris, 2019). However, when the analysis was recalculated using a simplified version of the VS model, working with more robust monthly data (Tolwinski-Ward et al., 2011), the overall pattern of results remained similar (Supporting Information Table S4).

The comparison of simulated and observed growth dynamics of *J. communis* at PEN site corroborates the evidence about the similarity between simulations and xylogenesis observations recently reported for trees (Buttò et al., 2020; Tumajer et al., 2021). In contrast, the simulated tracheid number and growth trends did not significantly reproduce means and trends in raw ring widths. This discrepancy can be attributed to the persistence of ontogenetic trends in raw chronologies (Fritts, 1976). Moreover, *J. communis* is known for irregular and strip bark growth around (Buras & Wilmking, 2014) and along (Shetti et al., 2018b) the stem. Consequently, trends and climatic signal of raw chronologies might be affected by the sampling position, orientation of radii and individual features, whereas trends in simulated chronologies reflect the overall effect of climatic conditions on the growth of a hypothetical average shrub free of dendrometric trends. In addition, *J. communis* is dioecious; hence, growth trends of raw chronologies obtained with a different sex ratio of sampled individuals might be affected by reproductive costs (Shetti et al., 2018a). Lastly, simulations calibrated against site chronologies must be interpreted as mean theoretical growth responses of entire shrub populations to the local climate. However, this might not hold at the level of individual shrubs if distinct subpopulations with diverging trends coexist. Growth divergence might have affected the common signal of site chronologies at the KIR and ABI sites, as indicated by the suboptimal mean inter-series correlation of raw series (Table 1).

4.3 | Importance of growth plasticity for the performance of the species across its distribution range

Our results highlight pronounced differences in simulated intra-annual growth of *J. communis* across the distributional range of the species. We revealed three distinct growth patterns typical for cold, dry and moist environments. Junipers are able to modify both their growth rates and the duration of the growing season in response to local climatic conditions, which has been recognized as an advantage for species expansion (Ghalambor et al., 2007). Indeed, *J. communis* has been able to develop viable metapopulations with sufficient fitness in contrasting environments and has become the most widespread woody plant across the globe (Adams, 2008). Moreover, simulated growth dynamics exhibit significant plasticity in response to climate change independent of the region, which increases the potential for expansion of the species and reduces the risk of local species extinction during periods of environmental change (Valladares et al., 2014). Accordingly, the expansion of *J. communis* to its current circumboreal area probably occurred quickly during Pliocene and Quaternary periods of climatic instability (Mao et al., 2010).

The extensive growth plasticity of *J. communis* might be a factor determining the potential for future expansion in cold regions and chances to survive in dry regions under ongoing climate change. Increasing summer growth rates in cold regions might be amplified by climate warming, further stimulating the elevational and latitudinal expansion of juniper populations (Hallinger et al., 2010; Myers-Smith et al., 2011). In contrast, the future survival of juniper shrubs in dry Mediterranean lowlands depends largely on the site-specific plasticity of growing season duration counterbalancing summer drought stress (Sánchez-Salguero & Camarero, 2020). Consequently, both northern and elevational tree lines together with dry shrublands might be expected to experience further shifts in cambial kinetics and phenology of *J. communis*. Owing to the already largely treeless composition of those ecosystems, the response of individual shrub species has the capacity to determine the overall future character of the entire landscape. However, given that intra-annual growth plasticity might differ between individual coexisting species, its assessment is required for additional species for predicting the landscape response to climate change.

As already stressed above, the climate-driven VS model revealed only the considered direct climatic effects on growth dynamics of *J. communis*. Although shrubs usually share a similar response to regional macroclimate, their local response might be modified by site-specific conditions (Buchwal et al., 2020). Indeed, the true local response of *J. communis* to future climate change might be shifted from our simulations by processes operating at the local scale, including indirect climatically triggered events (e.g., pathogen outbreaks, growth–reproduction trade-offs; Prendin et al., 2020; Shetti et al., 2018a), pollution (Kirdyanov et al., 2020), snow dynamics (Bjorkman et al., 2015; Pellizzari et al., 2014) or interactions between sympatric species (Sánchez-Salguero & Camarero, 2020). Although cambial activity is currently not assumed to be limited by the rate of photosynthesis even at the harshest sites (Körner, 2015), growth trends of *J. communis* populations might possibly decouple in the future from simulations in the event of significant increases of CO_2 concentrations and the potential of individual populations to adjust their rates of photosynthesis. Application of wood formation models other than sink-oriented would be required for the assessment of the growth response to trends in CO_2 concentration and additional processes not considered mechanistically by the VS model (Guiot et al., 2014).

4.4 | Conclusions

The VS model revealed regional differences in intra-annual patterns of *J. communis* growth dynamics and in the response to ongoing climate change. Specifically, *J. communis* occupies three climatically contrasting environments, with the dominance of limitation by cold (Arctic and Polar and Northern Urals), drought (Mediterranean and Southern Ural) or high soil moisture (Eastern Alps) on the growth dynamics during the main part of the growing season. Considering the wide distribution of the species, we can report that the adaptive and plastic growth dynamics were largely dependent on regional climate change. Although simulations suggest that shifting phenology is the dominant regional response of junipers to climate change in the dry environments (growing longer, but not faster), the trend towards increasing summer growth rates was simulated in cold environments (growing faster, but not for longer). Although the VS model proved to be an efficient tool to describe the overall effect of macroclimate on regional growth of *J. communis*, the suboptimal performance and non-stationarity observed in the Alps highlight that it might fail to reflect the processes altering the response to climate change at local scales.

Our results provide new insight into the spatial and temporal growth variability of the woody plant with the widest global distribution. The high simulated plasticity of growth dynamics might constitute a crucial predisposition that enabled *J. communis* to colonize a large geographical area and to survive under or even benefit from environmental instability. The assessment of intra-annual growth plasticity for other widespread woody species will extend our understanding of biogeographical patterns and ecosystem dynamics.

ACKNOWLEDGMENTS

J.T. was supported by an Alexander von Humboldt Research Fellowship. Fieldwork was enabled thanks to following funding sources: the European Union's Horizon 2020 project INTERACT, under grant agreements no. 262693 and no. 730938; TreeClim ERA.Net RUS Pilot Joint Call for Collaborative S&T Projects (funded under the 7th European Framework Programme for Research and Development); the Russian Scientific Foundation (grant no. RSF-17-14-01112). J.J.C. acknowledges the support in the field and the laboratory of A. Gazol and P. Moiseev. G.S.-B. is supported by a Spanish Ministry of Economy, Industry and Competitiveness Postdoctoral grant (FJCI 2016-30121; FEDER funds). J.A. was supported by research grants 20-05840Y of the Czech Science Foundation, INTER-EXCELLENCE LTAUSA19137 provided by Czech Ministry of Education, Youth and Sports, and long-term research development project RVO 67985939 of the Institute of Botany of the Czech Academy of Sciences. J.L. was supported by the project SURTUR: UJEP-SGS-2020-44-003-3 of the Jan Evangelista Purkyně University. We are grateful to Fred Rooks for improving the English language, Vladimir V. Shishov and Kevin Anchukaitis for making their implementations of the Vaganov–Shashkin model freely available, and three anonymous reviewers for stimulating comments on an earlier version of the manuscript.

CONFLICT OF INTEREST

The authors declare no conflict of interests.

AUTHOR CONTRIBUTIONS

J.T. and J.L. designed the research; A.B., J.J.C., M.C., J.L., R.S., G.S.-B. and M.W. collected data in the field and led their laboratory processing; J.L. compiled the database of all juniper ring-width series; and J.T. performed statistical analyses and led the writing of the paper with significant contribution of all co-authors.

DATA AVAILABILITY STATEMENT

Raw ring-width chronologies and simulation outputs for individual sites are available from the Dryad repository (https://doi.org/10.5061/dryad.cc2fqz659). We used implementations of the Vaganov–Shashkin model made available by Shishov et al. (2016; http://www.vs-genn.ru/) and Anchukaitis et al. (2020; https://github.com/kanchukaitis/vsm); the latter we forked and adjusted to be consistent with the former (https://github.com/jantumajer/vsm). Daily CRU JRA 1.1 climatic data are available from the CEDA Archive (https://catalogue.ceda.ac.uk/uuid/13f3635174794bb98cf8ac4b0ee8f4ed).

ORCID

Jan Tumajer https://orcid.org/0000-0002-7773-7081
Allan Buras https://orcid.org/0000-0003-2179-0681
J. Julio Camarero https://orcid.org/0000-0003-2436-2922
Rohan Shetti https://orcid.org/0000-0002-2967-0193
Martin Wilmking https://orcid.org/0000-0003-4964-2402
Jan Altman https://orcid.org/0000-0003-4879-5773
Gabriel Sangüesa-Barreda https://orcid.org/0000-0002-7722-2424
Jiří Lehejček https://orcid.org/0000-0001-8459-1028

REFERENCES

Adams, R. P. (2008). *Junipers of the world: The genus Juniperus*. Trafford Publishing.

Anchukaitis, K. J., Evans, M. N., Hughes, M. K., & Vaganov, E. A. (2020). An interpreted language implementation of the Vaganov–Shashkin tree-ring proxy system model. *Dendrochronologia*, *60*, 125677. https://doi.org/10.1016/j.dendro.2020.125677

Anchukaitis, K. J., Evans, M. N., Kaplan, A., Vaganov, E. A., Hughes, M. K., Grissino-Mayer, H. D., & Cane, M. A. (2006). Forward modeling of regional scale tree-ring patterns in the southeastern United States and the recent influence of summer drought. *Geophysical Research Letters*, *33*, L04705. https://doi.org/10.1029/2005GL025050

Babst, F., Bouriaud, O., Poulter, B., Trouet, V., Girardin, M. P., & Frank, D. C. (2019). Twentieth century redistribution in climatic drivers of global tree growth. *Science Advances*, *5*, eaat4313. https://doi.org/10.1126/sciadv.aat4313

Babst, F., Poulter, B., Trouet, V., Tan, K., Neuwirth, B., Wilson, R., Carrer, M., Grabner, M., Tegel, W., Levanic, T., Panayotov, M., Urbinati, C., Bouriaud, O., Ciais, P., & Frank, D. (2013). Site- and species-specific responses of forest growth to climate across the European continent. *Global Ecology and Biogeography*, *22*, 706–717. https://doi.org/10.1111/geb.12023

Bjorkman, A. D., Elmendorf, S. C., Beamish, A. L., Vellend, M., & Henry, G. H. R. (2015). Contrasting effects of warming and increased snowfall on Arctic tundra plant phenology over the past two decades. *Global Change Biology*, *21*, 4651–4661. https://doi.org/10.1111/gcb.13051

Buchwal, A., Sullivan, P. F., Macias-Fauria, M., Post, E., Myers-Smith, I. H., Stroeve, J. C., Blok, D., Tape, K. D., Forbes, B. C., Ropars, P., Lévesque, E., Elberling, B., Angers-Blondin, S., Boyle, J. S., Boudreau, S., Boulanger-Lapointe, N., Gamm, C., Hallinger, M., Rachlewicz, G., … Welker, J. M. (2020). Divergence of Arctic shrub growth associated with sea ice decline. *Proceedings of the National Academy of Sciences USA*, *117*, 33334–33344. https://doi.org/10.1073/pnas.2013311117

Buermann, W., Bikash, P. R., Jung, M., Burn, D. H., & Reichstein, M. (2013). Earlier springs decrease peak summer productivity in North American boreal forests. *Environmental Research Letters*, *8*, 024027. https://doi.org/10.1088/1748-9326/8/2/024027

Bunn, A. G. (2008). A dendrochronology program library in R (dplR). *Dendrochronologia*, *26*, 115–124. https://doi.org/10.1016/j.dendro.2008.01.002

Büntgen, U., Urban, O., Krusic, P. J., Rybníček, M., Kolář, T., Kyncl, T., Ač, A., Koňasová, E., Čáslavský, J., Esper, J., Wagner, S., Saurer, M., Tegel, W., Dobrovolný, P., Cherubini, P., Reinig, F., & Trnka, M. (2021). Recent European drought extremes beyond Common Era background variability. *Nature Geoscience*, *14*(4), 190–196. https://doi.org/10.1038/s41561-021-00698-0

Buras, A., & Wilmking, M. (2014). Straight lines or eccentric eggs? A comparison of radial and spatial ring width measurements and its implications for climate transfer functions. *Dendrochronologia*, *32*, 313–326. https://doi.org/10.1016/j.dendro.2014.07.002

Buras, A., Zang, C., & Menzel, A. (2017). Testing the stability of transfer functions. *Dendrochronologia*, *42*, 56–62. https://doi.org/10.1016/j.dendro.2017.01.005

Buttò, V., Shishov, V., Tychkov, I., Popkova, M., He, M., Rossi, S., Deslauriers, A., & Morin, H. (2020). Comparing the cell dynamics of tree-ring formation observed in microcores and as predicted by the Vaganov–Shashkin model. *Frontiers in Plant Science*, *11*, 1–16. https://doi.org/10.3389/fpls.2020.01268

Caldeira, M. C., Lecomte, X., David, T. S., Pinto, J. G., Bugalho, M. N., & Werner, C. (2015). Synergy of extreme drought and shrub invasion reduce ecosystem functioning and resilience in water-limited climates. *Scientific Reports*, *5*, 15110. https://doi.org/10.1038/srep15110

Camarero, J. J., Olano, J. M., & Parras, A. (2010). Plastic bimodal xylogenesis in conifers from continental Mediterranean climates. *New Phytologist*, *185*, 471–480. https://doi.org/10.1111/j.1469-8137.2009.03073.x

Carrer, M., Pellizzari, E., Prendin, A. L., Pividori, M., & Brunetti, M. (2019). Winter precipitation – not summer temperature – is still the main driver for Alpine shrub growth. *Science of the Total Environment*, *682*, 171–179. https://doi.org/10.1016/j.scitotenv.2019.05.152

Caudullo, G., Welk, E., & San-Miguel-Ayanz, J. (2017). Chorological maps for the main European woody species. *Data in Brief*, *12*, 662–666. https://doi.org/10.1016/j.dib.2017.05.007

Chae, Y., Kang, S. M., Jeong, S. J., Kim, B., & Frierson, D. M. W. (2015). Arctic greening can cause earlier seasonality of Arctic amplification. *Geophysical Research Letters*, *42*, 536–541. https://doi.org/10.1002/2014GL061841

Cook, E. R., & Peters, K. (1981). The smoothing spline: A new approach to standardizing forest interior tree-ring width series for dendroclimatic studies. *Tree-Ring Bulletin*, *41*, 45–53.

Cook, E. R., Solomina, O., Matskovsky, V., Cook, B. I., Agafonov, L., Berdnikova, A., Dolgova, E., Karpukhin, A., Knysh, N., Kulakova, M., Kuznetsova, V., Kyncl, T., Kyncl, J., Maximova, O., Panyushkina, I., Seim, A., Tishin, D., Ważny, T., & Yermokhin, M. (2020). The European Russia drought atlas (1400–2016 CE). *Climate Dynamics*, *54*, 2317–2335. https://doi.org/10.1007/s00382-019-05115-2

Cuny, H. E., Rathgeber, C. B. K., Frank, D., Fonti, P., Mäkinen, H., Prislan, P., Rossi, S., del Castillo, E. M., Campelo, F., Vavrčík, H., Camarero, J. J., Bryukhanova, M. V., Jyske, T., Gričar, J., Gryc, V., De Luis, M., Vieira, J., Čufar, K., Kirdyanov, A. V., … Fournier, M. (2015). Woody biomass production lags stem-girth increase by over one month in coniferous forests. *Nature Plants*, *1*, 15160. https://doi.org/10.1038/nplants.2015.160

D'Arrigo, R., Wilson, R., Liepert, B., & Cherubini, P. (2008). On the 'divergence problem' in northern forests: A review of the tree-ring evidence and possible causes. *Global and Planetary Change*, *60*, 289–305. https://doi.org/10.1016/j.gloplacha.2007.03.004

Delpierre, N., Lireux, S., Hartig, F., Camarero, J. J., Cheaib, A., Čufar, K., Cuny, H., Deslauriers, A., Fonti, P., Gričar, J., Huang, J., Krause, C., Liu, G., de Luis, M., Mäkinen, H., Martinez del Castillo, E., Morin, H., Nöjd, P., Oberhuber, W., … Rathgeber, C. B. K. (2019). Chilling and forcing temperatures interact to predict the onset of wood formation in Northern Hemisphere conifers. *Global Change Biology*, *25*, 1089–1105. https://doi.org/10.1111/gcb.14539

Evans, M. N., Reichert, B. K., Kaplan, A., Anchukaitis, K. J., Vaganov, E. A., Hughes, M. K., & Cane, M. A. (2006). A forward modeling approach to paleoclimatic interpretation of tree-ring data. *Journal of Geophysical Research*, *111*, G03008. https://doi.org/10.1029/2006JG000166

Frank, D. C., Poulter, B., Saurer, M., Esper, J., Huntingford, C., Helle, G., Treydte, K., Zimmermann, N. E., Schleser, G H, Ahlström, A., Ciais, P., Friedlingstein, P., Levis, S., Lomas, M., Sitch, S., Viovy, N., Andreu-Hayles, L., Bednarz, Z., Berninger, F., … Weigl, M. (2015). Water-use efficiency and transpiration across European forests during the Anthropocene. *Nature Climate Change*, *5*, 579–583. https://doi.org/10.1038/nclimate2614

Fritts, H. C. (1976). *Tree rings and climate*. Academic Press.

Froelich, N., Croft, H., Chen, J. M., Gonsamo, A., & Staebler, R. M. (2015). Trends of carbon fluxes and climate over a mixed temperate–boreal transition forest in southern Ontario, Canada. *Agricultural and Forest Meteorology*, *211–212*, 72–84. https://doi.org/10.1016/j.agrformet.2015.05.009

García-Cervigón Morales, A. I., Olano Mendoza, J. M., Eugenio Gozalbo, M., & Camarero, J. J. (2012). Arboreal and prostrate conifers coexisting in Mediterranean high mountains differ in their climatic responses. *Dendrochronologia*, *30*, 279–286. https://doi.org/10.1016/j.dendro.2012.02.004

Ghalambor, C. K., McKay, J. K., Carroll, S. P., & Reznick, D. N. (2007). Adaptive versus non-adaptive phenotypic plasticity and the potential for contemporary adaptation in new environments. *Functional Ecology*, *21*, 394–407. https://doi.org/10.1111/j.1365-2435.2007.01283.x

Guiot, J., Boucher, E., & Gea-Izquierdo, G. (2014). Process models and model-data fusion in dendroecology. *Frontiers in Ecology and Evolution*, *2*, 1–12. https://doi.org/10.3389/fevo.2014.00052

Hagedorn, F., Shiyatov, S. G., Mazepa, V. S., Devi, N. M., Grigor'ev, A. A., Bartysh, A. A., Fomin, V. V., Kapralov, D. S., Terent'ev, M., Bugman, H., Rigling, A., & Moiseev, P. A. (2014). Treeline advances along the Urals mountain range – driven by improved winter conditions? *Global Change Biology*, *20*, 3530–3543. https://doi.org/10.1111/gcb.12613

Hallinger, M., Manthey, M., & Wilmking, M. (2010). Establishing a missing link: Warm summers and winter snow cover promote shrub expansion into alpine tundra in Scandinavia. *New Phytologist*, *186*, 890–899. https://doi.org/10.1111/j.1469-8137.2010.03223.x

Harris, I. (2019). *CRU JRA v1.1: A forcings dataset of gridded land surface blend of Climatic Research Unit (CRU) and Japanese reanalysis (JRA) data*. Centre for Environmental Data Analysis.

Harvey, J. E., Smiljanić, M., Scharnweber, T., Buras, A., Cedro, A., Cruz-García, R., Drobyshev, I., Janecka, K., Jansons, Ā., Kaczka, R., Klisz, M., Läänelaid, A., Matisons, R., Muffler, L., Sohar, K., Spyt, B., Stolz, J., Maaten, E., Maaten-Theunissen, M., … Wilmking, M. (2020). Tree growth influenced by warming winter climate and summer moisture availability in northern temperate forests. *Global Change Biology*, *26*, 2505–2518.

Hu, J., Moore, D. J. P., Burns, S. P., & Monson, R. K. (2010). Longer growing seasons lead to less carbon sequestration by a subalpine forest. *Global Change Biology*, *16*, 771–783. https://doi.org/10.1111/j.1365-2486.2009.01967.x

Kirdyanov, A. V., Krusic, P. J., Shishov, V. V., Vaganov, E. A., Fertikov, A. I., Myglan, V. S., Barinov, V. V., Browse, J., Esper, J., Ilyin, V. A., Knorre, A. A., Korets, M. A., Kukarskikh, V. V., Mashukov, D. A., Onuchin, A. A., Piermattei, A., Pimenov, A. V., Prokushkin, A. S., Ryzhkova, V. A., … Büntgen, U. (2020). Ecological and conceptual consequences of Arctic pollution. *Ecology Letters*, *23*, 1827–1837. https://doi.org/10.1111/ele.13611

Körner, C. (2012). Treelines will be understood once the functional difference between a tree and a shrub is. *Ambio*, *41*, 197–206. https://doi.org/10.1007/s13280-012-0313-2

Körner, C. (2015). Paradigm shift in plant growth control. *Current Opinion in Plant Biology*, *25*, 107–114. https://doi.org/10.1016/j.pbi.2015.05.003

Mäkinen, H., Nöjd, P., Kahle, H.-P., Neumann, U., Tveite, B., Mielikäinen, K., Röhle, H., & Spiecker, H. (2002). Radial growth variation of Norway spruce (*Picea abies* (L.) Karst.) across latitudinal and altitudinal gradients in central and northern Europe. *Forest Ecology and Management*, *171*, 243–259. https://doi.org/10.1016/S0378-1127(01)00786-1

Mao, K., Hao, G., Liu, J., Adams, R. P., & Milne, R. I. (2010). Diversification and biogeography of *Juniperus* (Cupressaceae): Variable diversification rates and multiple intercontinental dispersals. *New Phytologist*, *188*, 254–272. https://doi.org/10.1111/j.1469-8137.2010.03351.x

McLean, E. H., Prober, S. M., Stock, W. D., Steane, D. A., Potts, B. M., Vaillancourt, R. E., & Byrne, M. (2014). Plasticity of functional traits varies clinically along a rainfall gradient in *Eucalyptus tricarpa*. *Plant, Cell & Environment*, *37*, 1440–1451.

Menzel, A., Sparks, T. H., Estrella, N., Koch, E., Aassa, A., Ahas, R., Alm-Kübler, K., Bissolli, P., Braslavská, O., Briede, A., Chmielewski, F. M., Crepinsek, Z., Curnel, Y., Dahl, Å., Defila, C., Donnelly, A., Filella, Y., Jatczak, K., Mage, F., … Zust, A. (2006). European phenological response to climate change matches the warming pattern. *Global Change Biology*, *12*, 1969–1976. https://doi.org/10.1111/j.1365-2486.2006.01193.x

Montserrat-Martí, G., Palacio, S., Milla, R., & Giménez-Benavides, L. (2011). Meristem growth, phenology, and architecture in chamaephytes of the Iberian Peninsula: Insights into a largely neglected life form. *Folia Geobotanica*, *46*, 117–136. https://doi.org/10.1007/s12224-010-9073-6

Myers-Smith, I. H., Forbes, B. C., Wilmking, M., Hallinger, M., Lantz, T., Blok, D., Tape, K. D., Macias-Fauria, M., Sass-Klaassen, U., Lévesque, E., Boudreau, S., Ropars, P., Hermanutz, L., Trant, A., Collier, L. S., Weijers, S., Rozema, J., Rayback, S. A., Schmidt, N. M., … Hik, D. S. (2011). Shrub expansion in tundra ecosystems: Dynamics, impacts and research priorities. *Environmental Research Letters*, *6*, 045509. https://doi.org/10.1088/1748-9326/6/4/045509

Oishi, A. C., Oren, R., Novick, K. A., Palmroth, S., & Katul, G. G. (2010). Interannual invariability of forest evapotranspiration and its consequence to water flow downstream. *Ecosystems*, *13*, 421–436. https://doi.org/10.1007/s10021-010-9328-3

Pallardy, S. G. (2008). *Physiology of woody plants*. Elsevier.

Payette, S., & Filion, L. (1985). White spruce expansion at the tree line and recent climatic change. *Canadian Journal of Forest Research*, *15*, 241–251. https://doi.org/10.1139/x85-042

Pellizzari, E., Camarero, J. J., Gazol, A., Granda, E., Shetti, R., Wilmking, M., Moiseev, P., Pividori, M., & Carrer, M. (2017). Diverging shrub and tree growth from the Polar to the Mediterranean biomes across the European continent. *Global Change Biology*, *23*, 3169–3180. https://doi.org/10.1111/gcb.13577

Pellizzari, E., Pividori, M., & Carrer, M. (2014). Winter precipitation effect in a mid-latitude temperature-limited environment: The case of common juniper at high elevation in the Alps. *Environmental Research Letters*, *9*, 104021. https://doi.org/10.1088/1748-9326/9/10/104021

Peltier, D. M. P., Barber, J. J., & Ogle, K. (2018). Quantifying antecedent climatic drivers of tree growth in the Southwestern US. *Journal of Ecology*, *106*, 613–624.

Peñuelas, J., Rutishauser, T., & Filella, I. (2009). Phenology feedbacks on climate change. *Science*, *324*, 887–888. https://doi.org/10.1126/science.1173004

Prendin, A. L., Carrer, M., Karami, M., Hollesen, J., Bjerregaard Pedersen, N., Pividori, M., Treier, U. A., Westergaard-Nielsen, A., Elberling, B., & Normand, S. (2020). Immediate and carry-over effects of insect outbreaks on vegetation growth in West Greenland assessed from cells to satellite. *Journal of Biogeography*, *47*, 87–100. https://doi.org/10.1111/jbi.13644

Prislan, P., Gričar, J., Čufar, K., de Luis, M., Merela, M., & Rossi, S. (2019). Growing season and radial growth predicted for *Fagus sylvatica* under climate change. *Climatic Change*, *153*, 181–197. https://doi.org/10.1007/s10584-019-02374-0

R Core Team (2020). *R: A language and environment for statistical computing*. R Foundation for Statistical Computing.

Rathgeber, C. B. K., Cuny, H. E., & Fonti, P. (2016). Biological basis of tree-ring formation: A crash course. *Frontiers in Plant Science*, *7*, 1–7. https://doi.org/10.3389/fpls.2016.00734

Rehfeldt, G. E., Wykoff, W. R., & Ying, C. C. (2001). Physiologic plasticity, evolution, and impacts of a changing climate on *Pinus contorta*. *Climatic Change*, *50*, 355–376.

Richardson, A. D., Hollinger, D. Y., Dail, D. B., Lee, J. T., Munger, J. W., & O'Keefe, J. (2009). Influence of spring phenology on seasonal and annual carbon balance in two contrasting New England forests. *Tree Physiology*, *29*, 321–331. https://doi.org/10.1093/treephys/tpn040

Rokach, L., & Maimon, O. (2005). Clustering methods. In O. Maimon & L. Rokach (Eds.), *The data mining and knowledge discovery handbook* (pp. 321–352). Springer.

Rossi, S., Anfodillo, T., Čufar, K., Cuny, H. E., Deslauriers, A., Fonti, P., Frank, D., Gričar, J., Gruber, A., Huang, J.-G., Jyske, T., Kašpar, J., King, G., Krause, C., Liang, E., Mäkinen, H., Morin, H., Nöjd, P., Oberhuber, W., … Treml, V. (2016). Pattern of xylem phenology in conifers of cold ecosystems at the Northern Hemisphere. *Global Change Biology*, *22*, 3804–3813. https://doi.org/10.1111/gcb.13317

Rossi, S., Deslauriers, A., Anfodillo, T., & Carraro, V. (2007). Evidence of threshold temperatures for xylogenesis in conifers at high altitudes. *Oecologia*, *152*, 1–12. https://doi.org/10.1007/s00442-006-0625-7

Rossi, S., Deslauriers, A., Gričar, J., Seo, J. W., Rathgeber, C. B. K., Anfodillo, T., Morin, H., Levanic, T., Oven, P., & Jalkanen, R. (2008).

Critical temperatures for xylogenesis in conifers of cold climates. *Global Ecology and Biogeography*, *17*, 696–707. https://doi.org/10.1111/j.1466-8238.2008.00417.x

Sánchez-Salguero, R., & Camarero, J. J. (2020). Greater sensitivity to hotter droughts underlies juniper dieback and mortality in Mediterranean shrublands. *Science of the Total Environment*, *721*, 137599. https://doi.org/10.1016/j.scitotenv.2020.137599

Sánchez-Salguero, R., Camarero, J. J., Carrer, M., Gutiérrez, E., Alla, A. Q., Andreu-Hayles, L., Hevia, A., Koutavas, A., Martínez-Sancho, E., Nola, P., Papadopoulos, A., Pasho, E., Toromani, E., Carreira, J. A., & Linares, J. C. (2017). Climate extremes and predicted warming threaten Mediterranean Holocene firs forests refugia. *Proceedings of the National Academy of Sciences USA*, *114*, E10142–E10150. https://doi.org/10.1073/pnas.1708109114

Sass-Klaassen, U., Sabajo, C. R., & den Ouden, J. (2011). Vessel formation in relation to leaf phenology in pedunculate oak and European ash. *Dendrochronologia*, *29*, 171–175. https://doi.org/10.1016/j.dendro.2011.01.002

Schweingruber, F. H. (1996). *Tree-rings and environment*. Dendroecology, Swiss Federal Institute for Forest, Snow and Landscape Research.

Seftigen, K., Frank, D. C., Björklund, J., Babst, F., & Poulter, B. (2018). The climatic drivers of normalized difference vegetation index and tree-ring-based estimates of forest productivity are spatially coherent but temporally decoupled in Northern Hemispheric forests. *Global Ecology and Biogeography*, *27*, 1352–1365. https://doi.org/10.1111/geb.12802

Shetti, R., Buras, A., Smiljanic, M., Hallinger, M., Grigoriev, A. A., & Wilmking, M. (2018a). Does sex matter? Gender-specificity and its influence on site-chronologies in the common dioecious shrub *Juniperus communis*. *Dendrochronologia*, *49*, 118–126. https://doi.org/10.1016/j.dendro.2018.03.006

Shetti, R., Buras, A., Smiljanic, M., & Wilmking, M. (2018b). Climate sensitivity is affected by growth differentiation along the length of *Juniperus communis* L. shrub stems in the Ural Mountains. *Dendrochronologia*, *49*, 29–35. https://doi.org/10.1016/j.dendro.2018.02.006

Shishov, V. V., Tychkov, I. I., Popkova, M. I., Ilyin, V. A., Bryukhanova, M. V., & Kirdyanov, A. V. (2016). VS-oscilloscope: A new tool to parameterize tree radial growth based on climate conditions. *Dendrochronologia*, *39*, 42–50. https://doi.org/10.1016/j.dendro.2015.10.001

St. George, S., Meko, D. M., & Evans, M. N. (2008). Regional tree growth and inferred summer climate in the Winnipeg River basin, Canada, since AD 1783. *Quaternary Research*, *70*, 158–172. https://doi.org/10.1016/j.yqres.2008.04.009

Thomas, P. A., El-Barghathi, M., & Polwarth, A. (2007). Biological flora of the British Isles: *Juniperus communis* L. *Journal of Ecology*, *95*, 1404–1440. https://doi.org/10.1111/j.1365-2745.2007.01308.x

Thornthwaite, C., & Mather, J. (1955). *The water balance. Publications in climatology (Vol. 1)*. Drexel Institute of Technology.

Tolwinski-Ward, S. E., Evans, M. N., Hughes, M. K., & Anchukaitis, K. J. (2011). An efficient forward model of the climate controls on interannual variation in tree-ring width. *Climate Dynamics*, *36*, 2419–2439. https://doi.org/10.1007/s00382-010-0945-5

Tumajer, J., Kašpar, J., Kuželová, H., Shishov, V. V., Tychkov, I. I., Popkova, M. I., Vaganov, E. A., & Treml, V. (2021). Forward modeling reveals multidecadal trends in cambial kinetics and phenology at treeline. *Frontiers in Plant Science*, *12*, 613646. https://doi.org/10.3389/fpls.2021.613643

Tychkov, I. I., Sviderskaya, I. V., Babushkina, E. A., Popkova, M. I., Vaganov, E. A., & Shishov, V. V. (2019). How can the parameterization of a process-based model help us understand real tree-ring growth? *Trees*, *33*, 345–357. https://doi.org/10.1007/s00468-018-1780-2

Vaganov, E. A., Hughes, M. K., & Shashkin, A. V. (2006). *Growth dynamics of conifer tree rings: Images of past and future environments*. Springer-Verlag.

Valladares, F., Matesanz, S., Guilhaumon, F., Araújo, M. B., Balaguer, L., Benito-Garzón, M., Cornwell, W., Gianoli, E., van Kleunen, M., Naya, D. E., Nicotra, A. B., Poorter, H., & Zavala, M. A. (2014). The effects of phenotypic plasticity and local adaptation on forecasts of species range shifts under climate change. *Ecology Letters*, *17*, 1351–1364. https://doi.org/10.1111/ele.12348

Vitasse, Y., Bresson, C. C., Kremer, A., Michalet, R., & Delzon, S. (2010). Quantifying phenological plasticity to temperature in two temperate tree species. *Functional Ecology*, *24*, 1211–1218. https://doi.org/10.1111/j.1365-2435.2010.01748.x

Weijers, S., Wagner-Cremer, F., Sass-Klaassen, U., Broekman, R., & Rozema, J. (2013). Reconstructing High Arctic growing season intensity from shoot length growth of a dwarf shrub. *The Holocene*, *23*, 721–731. https://doi.org/10.1177/0959683612470178

Wilmking, M., Buras, A., Lehejček, J., Lange, J., Shetti, R., & van der Maaten, E. (2018). Influence of larval outbreaks on the climate reconstruction potential of an Arctic shrub. *Dendrochronologia*, *49*, 36–43. https://doi.org/10.1016/j.dendro.2018.02.010

Xia, J., Niu, S., Ciais, P., Janssens, I. A., Chen, J., Ammann, C., Arain, A., Blanken, P. D., Cescatti, A., Bonal, D., Buchmann, N., Curtis, P. S., Chen, S., Dong, J., Flanagan, L. B., Frankenberg, C., Georgiadis, T., Gough, C. M., Hui, D., … Luo, Y. (2015). Joint control of terrestrial gross primary productivity by plant phenology and physiology. *Proceedings of the National Academy of Sciences USA*, *112*, 2788–2793. https://doi.org/10.1073/pnas.1413090112

Xu, C., Liu, H., Williams, A. P., Yin, Y., & Wu, X. (2016). Trends toward an earlier peak of the growing season in Northern Hemisphere mid-latitudes. *Global Change Biology*, *22*, 2852–2860. https://doi.org/10.1111/gcb.13224

Yang, B., He, M., Shishov, V., Tychkov, I., Vaganov, E. A., Rossi, S., Ljungqvist, F. C., Bräuning, A., & Grießinger, J. (2017). New perspective on spring vegetation phenology and global climate change based on Tibetan Plateau tree-ring data. *Proceedings of the National Academy of Sciences USA*, *114*, 6966–6971. https://doi.org/10.1073/pnas.1616608114

BIOSKETCH

The main research interest of the informal research group is the ecology of the most widespread woody species globally, *Juniperus communis*, in the European part of its distribution. Dendrochronology is the methodological approach most frequently adopted by the group members for the assessment of interactions between environmental conditions and juniper growth dynamics. The database of juniper ring-width chronologies, compiled and quality-checked by **Jiří Lehejček**, is based on data sampled and provided by individual group members.

SUPPORTING INFORMATION

Additional Supporting Information may be found online in the Supporting Information section.

How to cite this article: Tumajer, J., Buras A., Camarero J. J., Carrer M., Shetti R., Wilmking M., Altman J., Sangüesa-Barreda G., & Lehejček J. (2021). Growing faster, longer or both? Modelling plastic response of *Juniperus communis* growth phenology to climate change. *Global Ecology and Biogeography*, 30, 2229–2244. https://doi.org/10.1111/geb.13377